Environmental Science and Pollution Research (2023) 30:85223–85236
https://doi.org/10.1007/s11356-023-28083-x

RESEARCH ARTICLE

Effects of high $NaHCO_3$ alkalinity on growth, tissue structure, digestive enzyme activity, and gut microflora of grass carp juvenile

Jian Wen[1,2,3] · Song-lin Chen[1,2,3] · Wen-ya Xu[1,2,3] · Guo-dong Zheng[1,2,3] · Shu-ming Zou[1,2,3]

Received: 9 November 2022 / Accepted: 31 May 2023 / Published online: 29 June 2023

Abstract
With the gradual decrease in freshwater resources, the available space for freshwater aquaculture is diminishing. As a result, saline-alkaline water aquaculture has emerged as a crucial method to fulfill the increasing demand. This study investigates the impact of alkaline water on the growth performance, tissues (gill, liver, and kidney), digestive enzyme activity, and intestinal microbiology in grass carp (*Ctenopharyngodon idella*). The aquarium conditions were set with sodium bicarbonate (18 mmol/L (LAW), 32 mmol/L (HAW)) to simulate the alkaline water environment. A freshwater group was the control (FW). The experimental fish were cultured for 60 days. The findings revealed that $NaHCO_3$ alkaline stress significantly reduced growth performance, caused alterations in the structural morphology of gill lamellae, liver, and kidney tissues, and led to decreased activity of intestinal trypsin and lipase amylase ($P < 0.05$). Analysis of 16S rRNA sequences demonstrated that alkalinity influenced the abundance of dominant bacterial phyla and genera. Proteobacteria showed a significant decrease under alkaline conditions, while Firmicutes exhibited a significant increase ($P < 0.05$). Furthermore, alkalinity conditions significantly reduced the abundance of bacteria involved in protein, amino acid, and carbohydrate metabolism, cell transport, cell decomposition, and environmental information processing. Conversely, the abundance of bacteria associated with lipid metabolism, energy metabolism, organic systems, and disease functional flora increased significantly under alkalinity conditions ($P < 0.05$). In conclusion, this comprehensive study indicates that alkalinity stress adversely affected the growth performance of juvenile grass carp, likely due to tissue damage, reduced activity of intestinal digestive enzymes, and alterations in intestinal microorganisms.

Keywords Grass carp · $NaHCO_3$ · Growth performance · Digestive enzyme activity · Gut microflora

Introduction

As one of the most representative herbivorous fish in China, grass carp (*Ctenopharyngodon idella*) is renowned for its delicious meat and rich nutritional value (Yang et al. 2020). Although China possesses abundant water resources, there are still numerous low-lying saline waters that remain underutilized (Yao et al. 2015). Research has shown that high alkalinity can damage tissue structures and have a significant impact on the growth, reproduction, physiology, and biochemistry of aquatic organisms (Yao et al. 2012).

Studies on saline-alkaline research in fish have primarily focused on growth, tolerance to saline-alkaline stress, nonspecific immune mechanisms, and transcriptomics (Chen et al. 2020). Alkalinity stress stimulates energy and ion regulation pathways, while slowing down pathways related to the immune system and reproduction (Yao et al. 2012). Research has demonstrated that

Responsible Editor: Bruno Nunes

Jian Wen and Song-lin Chen contributed equally to this work.

✉ Shu-ming Zou
smzou@shou.edu.cn

Guo-dong Zheng
gdzheng@shou.edu.cn

1 Genetics and Breeding Center for Blunt Snout Bream, Ministry of Agriculture and Rural Affairs, Shanghai Ocean University, Shanghai 201306, China

2 Key Laboratory of Freshwater Aquatic Genetic Resources, Ministry of Agriculture and Rural Affairs, Shanghai Ocean University, Shanghai 201306, China

3 National Demonstration Center for Experimental Fisheries Science Education, Shanghai Ocean University, Shanghai 201306, China

chronic stress can suppress the immune response, down-regulate normal immune responses, and increase the likelihood of disease contraction in *Triplophysa yarkandensis* subjected to salt-alkaline stress for 30 days (Chen et al. 2020). Similarly, under saline-alkaline stress, the expression level of osmoregulatory genes in Ridgetail white prawn (*Exopalaemon carinicauda*) is diminished (Ge et al. 2019).

Similar to most organisms, the intestinal tract of fish harbors a large number of microorganisms. The functions of fish intestinal flora primarily involve improving nutrition, enhancing immune regulation, and inhibiting pathogenic bacteria (Wu et al. 2012). The gut microbiota of fish performs a vital function through the secretion of protease, amylase, and lipase, which provide essential nutrients necessary for the fish's growth, development, and overall health (Hao et al. 2017a, b). Additionally, the fish's gut microbiota synthesizes a diverse array of vitamins, including vitamin B12, contributing to the digestion and absorption of nutrients (Hassenruck et al. 2020). Fish and their digestive tract microorganisms have developed a complex symbiotic relationship through mutual adaptation over an extended period of natural evolution (Sullam et al. 2012). The intestinal microorganisms play an irreplaceable role in nutrient absorption, intestinal immunity, and intestinal physiological regulation for the fish, which directly affects the host's dietary habits, growth performance, and immune function (Yi et al. 2019).

Several studies have revealed that probiotics have the ability to regulate weight and metabolic function by influencing food intake through the modulation of intestinal bacterial communities (Kobyliak et al. 2016). *Bacillus subtilis* can be used to promote intestinal health by regulating the immune response and fat metabolism in grass carp intestines, as observed in a study by Yaotong Hao (Hao et al. 2017a, b). The researchers observed that grass carp exhibited a higher abundance of functional microorganisms related to carbohydrate transport and metabolism in their intestines when fed Sudan grass. Conversely, when fed animal feed, an increase in the presence of bacteria associated with energy and protein metabolism was observed (Hao et al. 2017a, b).

Since no previous studies have examined the effects of alkalinity stress conditions on the growth performance, histomorphology, and gut microbial community structure of grass carp, our aim is to investigate these effects in juvenile grass carp under high alkalinity. To achieve this, we established three different alkalinity conditions (0, 18, 32 mmol/L) based on the maximum tolerated concentration of $NaHCO_3$ (37 mmol/L). This maximum tolerated concentration was determined through pre-experimental alkalinity tests conducted on grass carp juveniles.

Materials and methods

Experimental fish and daily management

The experimental grass carp juveniles were artificially bred at the fish breeding experimental station of Qingpu, which is part of the Aquatic Biogenetic Breeding Center at Shanghai Ocean University. A group of healthy juvenile grass carp, with a comparable size of 6.62 ± 1.32 g and 6.94 ± 0.56 cm ($n = 270$), was randomly selected and reared in a 1 m^3 container with blue plastic for a duration of 60 days. The experiment was divided into three groups, each consisting of three replicates, with each replicate stocked with 30 experimental fish. The fish were fed three times a day (08:00, 13:00, and 18:00) using Tong Wei small pellet floating feed, specifically designed for young fish (feed ingredients are shown in Table 1). In the actual breeding process, the experimental water underwent 72 h of aeration, and the experimental conditions were established using two concentrations of AW: 1.56 g/L (alkalinity = 18.57 mmol/L, pH 8.5 ± 0.1) and 2.73 g/L (alkalinity = 32.5 mmol/L, pH 8.9 ± 0.1). These concentrations were prepared by combining FW (alkalinity = 0.66 mmol/L, pH 7.3 ± 0.1) with sodium bicarbonate ($NaHCO_3$). The alkalinity was determined using acidimetric titrations and expressed in millimoles per liter (mmol/L).

The water temperature during the experiment ranged from 20 to 25 °C, with dissolved oxygen (DO) levels above 5.85 mg/L, NH_4^+-N levels below 0.5 mg/L, and NO_2-N levels below 0.05 mg/L. The intake of bait was recorded statistically for each group, and the survival rate of each group was calculated.

Processing of samples and data collection

At the conclusion of the culture experiment, the body length and body mass of all fish were measured. Additionally, the survival rate was determined after a 24-h fasting period. Juvenile grass carp were randomly selected from each parallel group and anesthetized in an MS-222 (200 mg/L) solution. Subsequently, they were dissected on ice (Song et al. 2021). Three fish from each parallel group had their gills, liver, and kidneys fixed in Bouin's solution for 24 h. Subsequently, they were stored in 70% alcohol for histological

Table 1 Formulation and proximate composition of commercial diets

Nutrients	Input (%)
Crude protein	32.0
Crude fiber	12.0
Crude fat	8.0
Crude ash	15.0
Lysine	1.4

and histochemical observation. Under aseptic conditions, the midgut and its contents were randomly extracted from each parallel group and placed into 1.5-mL centrifuge tubes. Subsequently, they were transferred to liquid nitrogen and stored at – 80 ℃ as a backup.

Growth index assessment

The growth performance of fish cultured for 60 days was evaluated based on several indicators, including survival rate (*SR*), weight gain rate (*WGR*), feed conversion ratio (*FCR*), and specific growth rate (*SGR*). The aforementioned indexes were calculated using the following equations.

$$SR(\%) = N_t/N_o \times 100\% \tag{1}$$

$$WGR(\%) = [(W_2 - W_1)/W_1] \times 100\% \tag{2}$$

$$FCR(g) = \left[W_f/(W_2 - W_1)\right] \tag{3}$$

$$SGR(\%/d) = [(lnW_2 - \ln W_1)/T] \times 100\% \tag{4}$$

Note: in the equation, "*No*" represents the initial number of fishtails counted, "*Nt*" represents the final number of fishtails counted. "*W1*" and "*W2*" represent the average initial and final body weight of each fish group, respectively. "*T*" represents the experimental time, and "*Wf*" represents the average food intake during the experiment.

Histological analysis

At the conclusion of the experiment, three fish were selected from each parallel group. The gill, liver, and kidney tissues were then fixed in Bouin's solution for 24 h after anesthetizing the test fish using MS-222. Following alcohol gradient dehydration, xylene transparency, paraffin wax permeation at 60 ℃, tissue embedding, and subsequent sectioning (at 5 μm), drying, H&E staining, neutral gum sealing, and other necessary procedures were conducted to prepare the paraffin sections. Finally, photos were captured using a Nikon Eclipse 80i light microscope.

Digestive enzyme activity assay

The entire procedure was conducted on ice, and the bowel was flushed with saline (0.7%). Next, 0.1 g of the sample was taken, homogenized according to the kit's instructions, and centrifuged for 15 min at 4 °C and 2500 revolutions per minute (rpm). The activities of amylase, lipase, and trypsin were determined from the supernatant. The activity values for each digestive enzyme in the samples were then calculated using the standard curve (the reagents were purchased from Nanjing Jiancheng Institute of Biological Engineering).

Sequencing of gut microbial samples

Total bacterial DNA was extracted from the microbial community of grass carp intestinal contents using the Fast DNA SPIN Kit for Feces (MPB biomedical). PCR amplification was performed with diluted genomic DNA as the template. Specific primers with barcodes were selected based on the amplification region. The amplification was carried out using Phusion High Fidelity PCR Master Mix with GC Buffer from New England Biolabs Company and Efficient transcriptase. The V4 region of the 16S rRNA gene was amplified using two universal primers: 515F (5′-GTGYCAGCMGCCGCGGTAA-3′) and 806R (5′-GGACTCANVGGGTWTCTAAT-3′). The Raw Tags obtained were subjected to quality control using fastp software, resulting in high-quality Clean Tags. These Clean Tags were then compared with a database using Usearch software to identify and remove chimeras, resulting in the generation of the final validated Effective Tags. The DADA2 algorithm in QIIME2 software was employed for noise reduction and filtering out sequences with an abundance less than 5, resulting in the generation of the final classification unit, Operational Taxonomic Units (OTUs).

Data analysis

The thickness, length, and spacing of gill lamellae, as well as the length of protruding gill lamellae and the thickness of interlamellar cell clusters, were measured and quantified using Image J software. The experimental data were expressed as "mean ± standard deviation" (mean ± SD), and the data were analyzed using SPSS22 software. One-way ANOVA was used to compare the significance of differences between the data at a significance level of $P = 0.05$. QIIME2 software was employed to calculate observed OTUs, Shannon, Simpson, Chao1, Goods, and coverage indices, as well as to plot dilution curves (Rarefaction Curve) and analyze the intergroup differences in the alpha diversity of the intestinal flora. The PICRUSt2 (Phylogenetic Investigation of Communities by Reconstruction of Unobserved Stats 2) platform is used to infer the gene functions of gut microbes in juvenile fish. This is done based on the OTU tree and the genetic information of OTUs obtained from the Greengene database. The top 24 flora richness values were selected for *Level 1*, *Level 2*, and *Level 3* analyses, and GraphPad Prism 8 software was utilized for graphing.

Results

Growth performance

At the beginning of the experiment, there were no significant differences in the initial weight, length and height of grass carp juvenile. There were no mortalities of fish in any of the groups in this experiment. From Table 2, it was obtained that the final weight, weight gain rate, and specific growth rate of the HAW group were significantly ($P<0.05$) lower than those of the LAW group, and extremely significant ($P<0.01$) lower than FW group. Final weight, weight gain rate, and specific growth rate were significantly lower in the LAW group than FW group. The final body length of the HAW group was significantly lower than FW group, but the LAW group was not significantly different from the FW group. Furthermore, the bait coefficient of the HAW group was significantly higher than that of the FW group ($P<0.01$), but no significant difference was observed between the HAW and LAW groups.

Morphology

As observed in Table 3, the length of gill lamellae in the FW and HAW groups was significantly shorter than that in the LAW group ($P<0.01$). Additionally, the length of gill lamellae in the HAW group was significantly shorter than that in the FW group ($P<0.01$). The PL in the FW and HAW groups was significantly shorter than that in the LAW group ($P<0.01$). Furthermore, the PL in the FW group was significantly shorter than that in the HAW group ($P<0.01$). The ILCM height was significantly lower in both the LAW and HAW groups compared to the FW group ($P<0.01$). The spacing of gill lamellae was significantly greater in the LAW group compared to both the FW and HAW groups, and the HAW group showed an extremely significant difference ($P<0.01$) with the FW group. The changes in the gill structure of grass carp juveniles in all experimental groups are shown in Fig. 1. The gill filament morphology of the FW group exhibited a normal structure of gill filaments. The gill filaments of the LAW group exhibited interlamellar cell loss and increased spacing between gill lamellae. A noticeable trend was observed from the LAW group to the HAW group, with gill lamellae and PL becoming progressively shorter. Additionally, there was evidence of necrotic epithelium sloughing in the gill lamellae, and the thinning of gill lamellae thickness was more pronounced.

The liver tissue of juvenile fish in the FW group exhibited a normal hepatocyte structure with uniform cytoplasm. Slight deviation of the nucleus from the center of the cell was observed (38.23 ± 8.7 cells/mm^2). In contrast, the nuclei of hepatocytes in the LAW (170.23 ± 8.7 cells/mm^2) and HAW (379 ± 9.2 cells/mm^2) groups showed a significant deviation from the center of the cell (arrow) compared to the FW group, indicating a pronounced increase with higher alkalinity ($P<0.01$). Furthermore, hepatocytes in the HAW group (190.40 ± 4.68 cells/mm^2) exhibited significant swelling compared to the FW group (124.43 ± 1.68 cells/mm^2) and LAW group (125.50 ± 2.48 cells/mm^2) ($P<0.01$). Cytoplasmic vacuolization was also observed in the HAW group (circles) (Fig. 2).

Observations revealed that the renal tubular lumen in the LAW group (triangular sign) was enlarged, while the renal tubular epithelial cells in the HAW group exhibited swelling and necrotic epithelium (arrows). Furthermore, the tubular lumen in the HAW group appeared to be even

Table 2 The growth parameters at different alkalinity groups during 60 days experiments

Indicators group	0 d		60 d		WGR/ %	SGR/ %/d	FCR/g
	Body length/cm	Body weight /g	Body length /cm	Body weight /g			
FW	6.94 ± 0.56^a	6.62 ± 1.32^a	10.73 ± 0.91^a	24.78 ± 2.34^a	275 ± 9.60^a	2.21 ± 0.19^a	1.91 ± 0.18^a
LAW	6.94 ± 0.56^a	6.62 ± 1.32^a	10.04 ± 0.87^a	21.09 ± 2.67^b	218 ± 10.20^b	1.93 ± 0.16^b	2.27 ± 0.14^b
HAW	6.94 ± 0.56^a	6.62 ± 1.32^a	9.55 ± 0.55^b	19.73 ± 3.21^c	198 ± 5.10^c	1.82 ± 0.29^c	2.52 ± 0.15^c

Values are means ± SD, ($n=30$). Different superscript letters in the same column indicate significant differences ($P<0.05$)

Table 3 Morphological characteristics of gill histology under alkalinity stress

Gill morphology measurements (μm)					
Group	Length of gill lamellae	Gill lamellae spacing	Thickness of gill lamellae	ILCM height	PL length
FW	126.34 ± 10.49^a	10.86 ± 1.17^a	21.12 ± 1.73^a	59.86 ± 3.51^a	59.77 ± 6.78^a
LAW	178.09 ± 14.47^b	22.15 ± 2.79^b	19.40 ± 3.21^b	47.03 ± 3.74^b	126.86 ± 7.32^b
HAW	118.45 ± 8.29^c	18.26 ± 2.22^c	11.81 ± 1.87^c	34.39 ± 3.62^b	81.6 ± 5.53^c

Values are means ± SD, ($n=30$). Letters over each column indicate significant differences ($P<0.05$)

Fig. 1 Effects of $NaHCO_3$ on gill structure (H&E staining, 400×). **a** FW group, **b** LAW group, **c** HAW group. I, thickness of gill lamella (μm); II, length extending from the base of gill lamella (μm); III, length of protruding gill lamellae (μm) (PL); IV, thickness of interlaminar matrix of gill lamella (μm); V, distance between two adjacent gill lamellae (μm). L, secondary lamellae; ILCM, interlayer cells mass

more prominently enlarged (triangular sign). In contrast, the cellular structures such as renal tubular epithelial cells and tubular lumen in the FW group (Fig. 3) remained unaffected.

Intestinal digestive enzyme activity

According to the data presented in Table 4, both the trypsin and lipase activities in the intestinal tissues of both the LAW and HAW groups were significantly lower ($P < 0.05$) compared to the FW group. Notably, as the alkalinity increased, there was a more pronounced decrease in enzyme activity. The amylase activity in the LAW group did not show a clear difference compared to the FW group, while the amylase activity in the HAW group was significantly lower than that in the FW group.

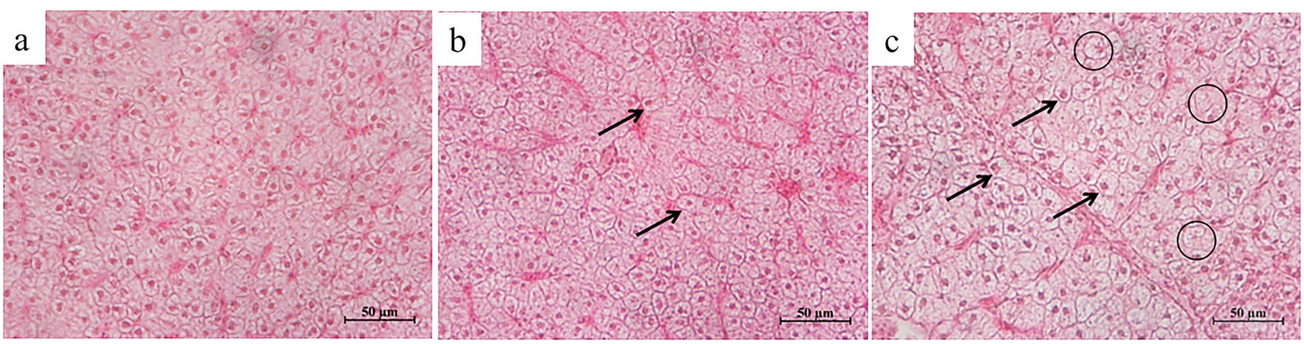

Fig. 2 Effects of $NaHCO_3$ on the structure of hepatocytes (H&E staining, 400×). **a** FW group, **b** LAW group, **c** HAW group; arrows, nucleus deviates from the center of the cell, circles, Cytoplasmic vacuolation

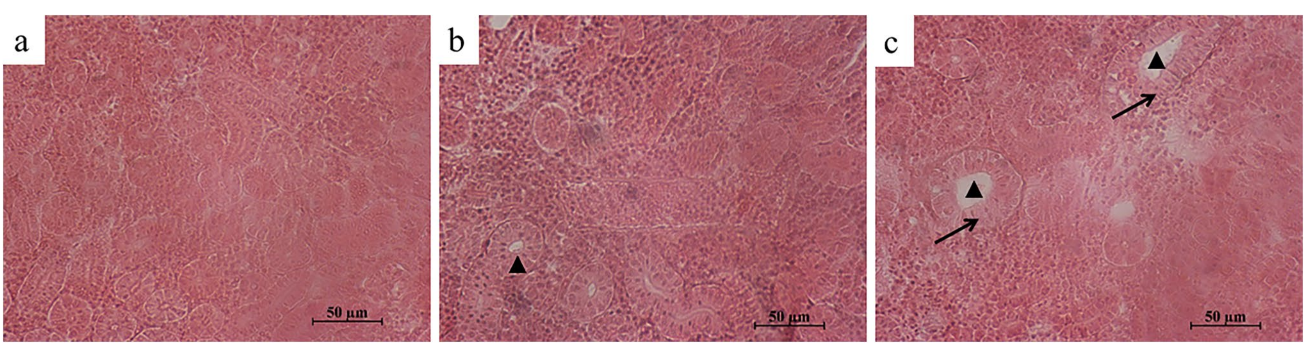

Fig. 3 Effects of $NaHCO_3$ on the structure of kidney cells (H&E staining, 400×). **a** FW group, **b** LAW group, **c** HAW group. Triangles, renal tubules with enlarged lumen; arrows, swollen, necrotic epithelium of renal tubular epithelial cells

Table 4 Digestive enzyme activity indexes

Parameter	FW	LAW	HAW
Trypsin (U/ mg)	2654.80 ± 87.74[a]	2349.70 ± 61.31[b]	2183.40 ± 80.89[c]
Lipase (U/ g)	241.03 ± 5.21[a]	226.90 ± 4.82[b]	216.20 ± 7.32[c]
Amylase (U/ mg)	434.50 ± 8.18[a]	431.70 ± 4.03[a]	419.10 ± 6.10[b]

Data are expressed as the means ± SD ($n = 9$). The letters on each line indicate a significant difference ($P < 0.05$)

OTU and Alpha diversity index of intestinal microorganisms

For this study, the V4 region of the 16S rRNA gene in juvenile fish was sequenced using the Illumina NovaSeq PE250 sequencing platform. A total of 974,299 raw reads were obtained, out of which 954,710 effective sequences were selected for subsequent analysis. Alpha diversity analysis indices are widely used to assess species abundance and diversity. The results of the alpha diversity analysis are presented in Table 5. There were no significant differences observed among the different groups in terms of the α-diversity index. However, both the Chao and Shannon indices exhibited a tendency to increase with higher alkalinity levels. Dilution curves were generated based on the measured valid data (Fig. 4). It is evident that the rarefaction curves of each group gradually level off, and the Good's coverage of each group approaches 1. This indicates that nearly all sequences in the samples have been detected, and the amount of sequencing data is relatively adequate. The HAW group exhibited the highest Shannon index, while the LAW group showed the highest Simpson diversity index (Fig. 4 and Table 5).

As shown in Venn Diagram (Fig. 5), there were 653 clusters in the FW group, 546 clusters in the LAW group, and 687 clusters in the HAW group. The number of OTUs specific to the FW and LAW groups was 418 and 311, respectively, while the total number of shared species between them was 235. There were 405 OTUs specific to the FW group and 439 OTUs specific to the HAW group, with a total of 248 species present in both groups. There were 267 OTUs specific to the LAW group and 408 OTUs specific to the HAW group, with a total of 279 species present in both groups. The three groups shared 13.87% of the OTUs in common, while the number of unique OTUs accounted for 26.9%, 16.32%, and 26.13% of the total in the three groups,

Table 5 Alpha diversity index of gut microbial

Indicators group	Chao 1 index	Shannon index	Simpson index	Good's coverage
FW	306.29 ± 96.11	3.90 ± 1.10	0.82 ± 0.12	1.00 ± 0.00
LAW	321.45 ± 28.83	4.24 ± 0.31	0.87 ± 0.02	1.00 ± 0.00
HAW	337.11 ± 131.76	4.37 ± 1.60	0.81 ± 0.18	1.00 ± 0.00

Values are means ± SD, $n = 3$

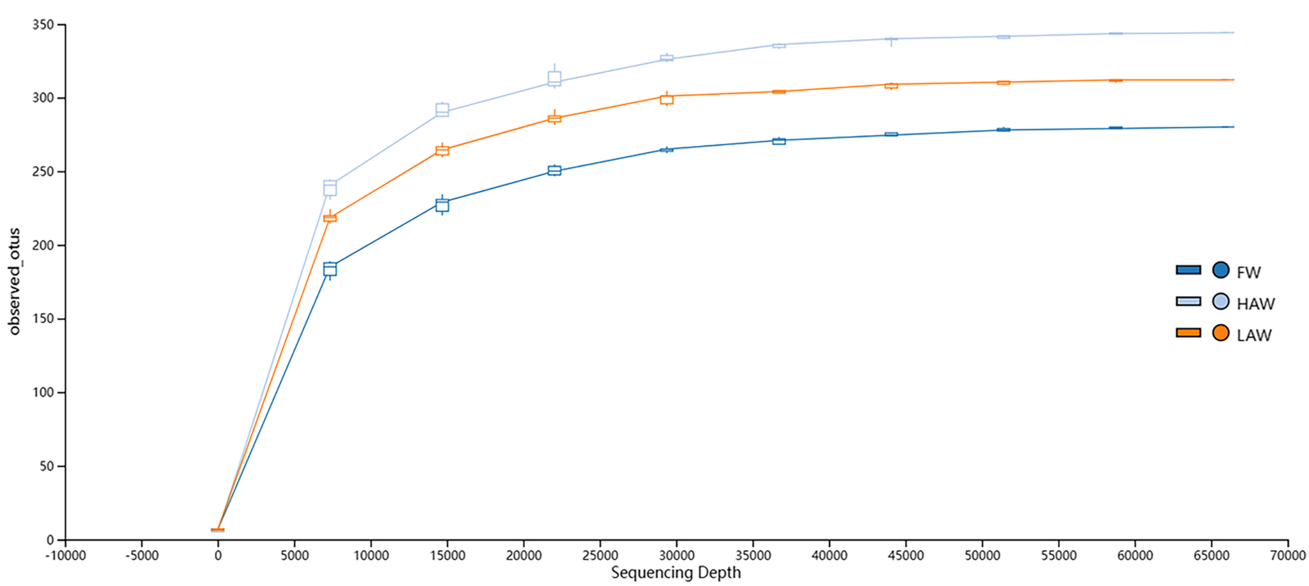

Fig. 4 Rarefaction curve

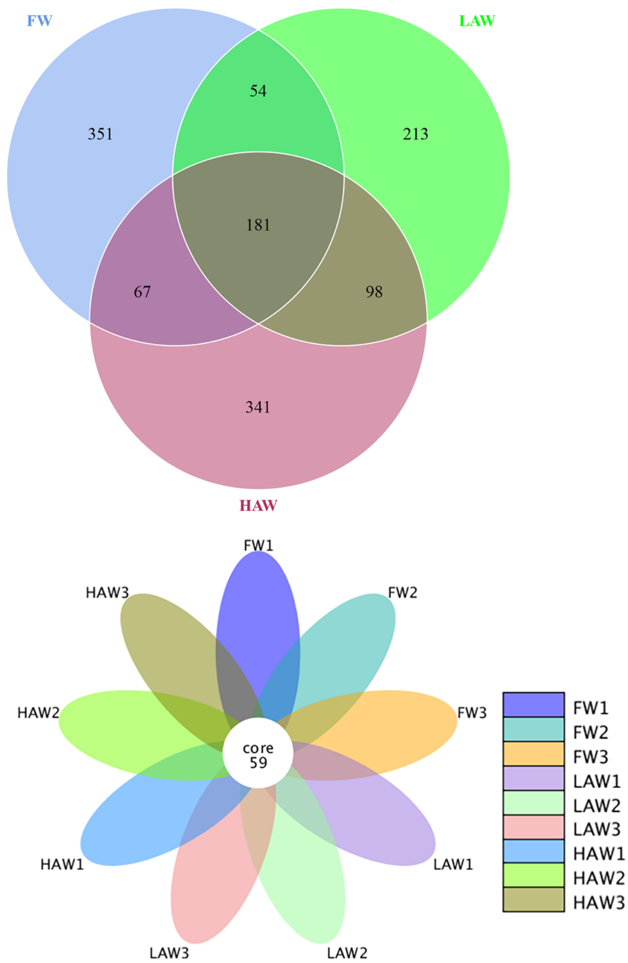

Fig. 5 Venn diagram comparing the observed OTU of intestinal bacterial communities

respectively. Compared to the FW group, the LAW group showed a reduction of 107 OTU clusters, while the HAW group exhibited an increase of 34 OTU clusters.

The composition of gut microbiome

To observe the structure of gut microorganisms in juvenile fish at different taxonomic levels, data from all groups of juvenile fish gut microorganisms were combined for comparative analysis using statistical methods. Microbial community structure can be analyzed at various taxonomic levels, including phylum, class, order, family, and genus. Currently, the most commonly performed analyses are at the phylum and genus levels. Species annotation analysis of the samples based on the phylum level revealed 24 microbial phyla in this experiment. The top 9 species in terms of abundance were selected to generate histograms, while the remaining species were combined as "Others." According to Fig. 6, the major bacterial phyla for the FW group were Fusobacteria (45.34%), Proteobacteria (35.95%), and Firmicutes (8.13%). Similarly, the LAW group had Fusobacteria (44.99%), Proteobacteria (24.06%), and Firmicutes (20.64%) as the major bacterial phyla. In contrast, the HAW group displayed Fusobacteria (41.41%), Proteobacteria (28.68%), and Firmicutes (19.65%) as the major bacterial phyla. It is evident that the dominant bacterial populations in the three alkalinity groups primarily belong to the phyla Fusobacteria, Proteobacteria, and Firmicutes. The three dominant phyla accounted for 89.41%, 89.69%, and 89.73% of the total gut microbiome in each respective group.

Based on the genera level, species annotation analysis was conducted on the samples, and histograms were generated using the top 11 species with the highest abundance, as shown in Fig. 7. *Cetobacterium* (57.49%), *Candidatus–Berkiella* (8.69%), and *Phreatobacter* (9.60%) were major microbial genus for the FW group. *Cetobacterium* (56.96%), *Bacteroides* (7.19%), and *Aeromonas* (2.99%) were major microbial genus for the LAW group. *Cetobacterium* (25.84%), *Sebaldella* (26.96%), and *Aeromonas* (8.67%) were major microbial genus for the HAW group.

Fig. 6 Histogram of the relative abundance of intestinal microbes at the phylum level

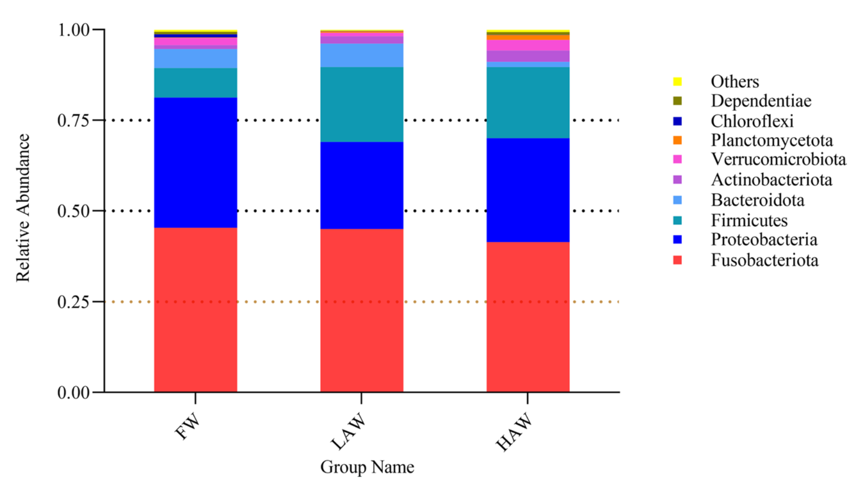

Fig. 7 Histogram of the relative abundance of intestinal microbes at the genus level

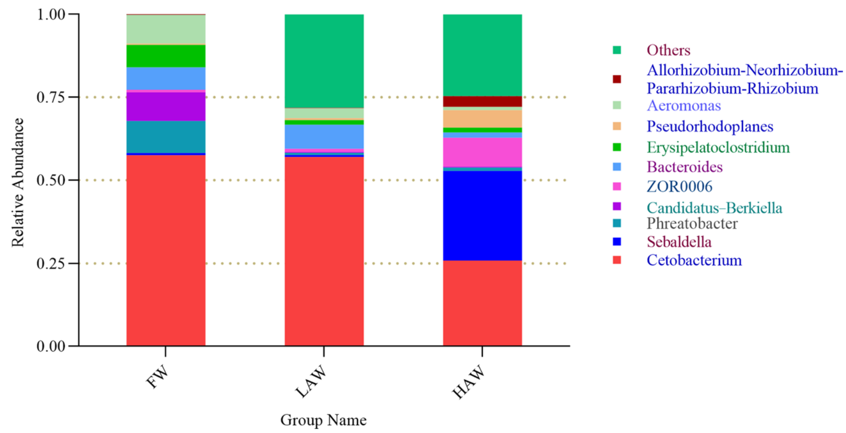

Function prediction of gut bacterial communities

To analyze functional differences based on COG (clusters of orthologous group) functional annotations and abundance information, the top 24 abundantly ranked samples were selected. A clustering analysis was performed at the functional level, and a heat map was generated to visualize the results. The experiment depicted in Fig. 8 yielded crucial conclusions. At *Level 1*, the abundance of functional flora involved in metabolism, genetic information processing, environmental information processing, and cellular transport and catabolism was lower in the LAW and HAW groups compared to the FW group. Furthermore, there was a decrease in the abundance of flora with increasing alkalinity. Both the LAW and HAW groups exhibited a higher abundance of organismal systems functional microflora and human diseases-related flora compared to the FW group.

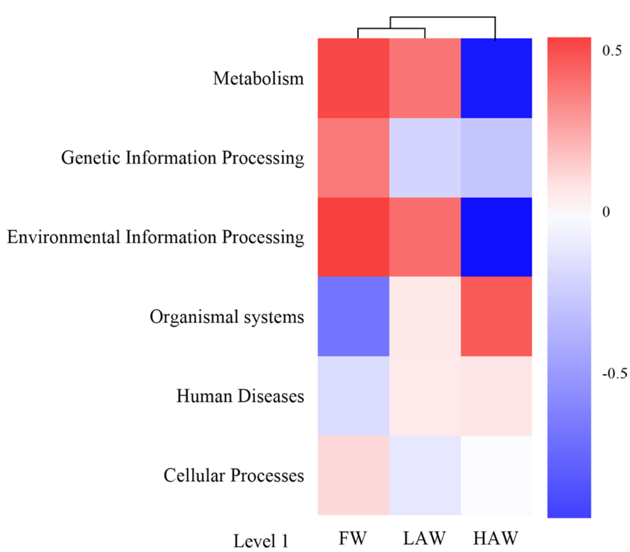

Fig. 8 Distribution of COG functional annotations feature heat maps (*Level 1*)

Additionally, the abundance of flora showed an increasing trend with rising alkalinity.

According to Fig. 9, at *Level 2* and *Level 3*, the abundance of functional flora related to energy metabolism was higher in the LAW and HAW groups compared to the FW group. The protein and amino acid metabolism in the LAW and HAW groups was lower than in the FW group, and the bacterial community abundance decreased with increasing alkalinity. The HAW group exhibited the highest abundance of ADP-glyceromanno heptose 6 epimerase activity and carbohydrate transport in the glucose metabolism microflora. The FW group, on the other hand, showed the highest abundance of transferase activity transferring glycosyl groups and ADP-heptose-lipopolysaccharide heptenyl transferase activity functional flora. Notably, the HAW group had the lowest abundance of these functions. In lipid metabolism, the LAW and HAW groups exhibited higher abundance of functional microflora involved in hydrolase activity-acting on ester bonds and Acyl-CoA dehydrogenase activity, compared to the FW group. Additionally, the abundance of functional flora involved in the purine nucleotide biosynthetic process, which is part of nucleotide metabolism, was higher in both the LAW and HAW groups compared to the FW group. The abundance of functional microflora involved in the genetic material information processing pathway (transcription) was lower in the LAW and HAW groups compared to the FW group, with the HAW group exhibiting the lowest abundance among the groups. The abundance of the phosphoenolpyruvate-dependent sugar phosphotransferase system in signaling molecular and interactions microflora was highest in the HAW group and lowest in the LAW group. The abundance of Na^+/H^+ antiporter, belonging to the membrane fusion protein (MFP) (TC8.A.1) family, was lower in the LAW and HAW groups compared to the FW group, with the lowest abundance observed in the HAW group. The abundance of drug transmembrane transporter active functional flora in the HAW group was lower than in the FW group, while the LAW group had the highest abundance. Additionally, the abundance of the functional microflora involved

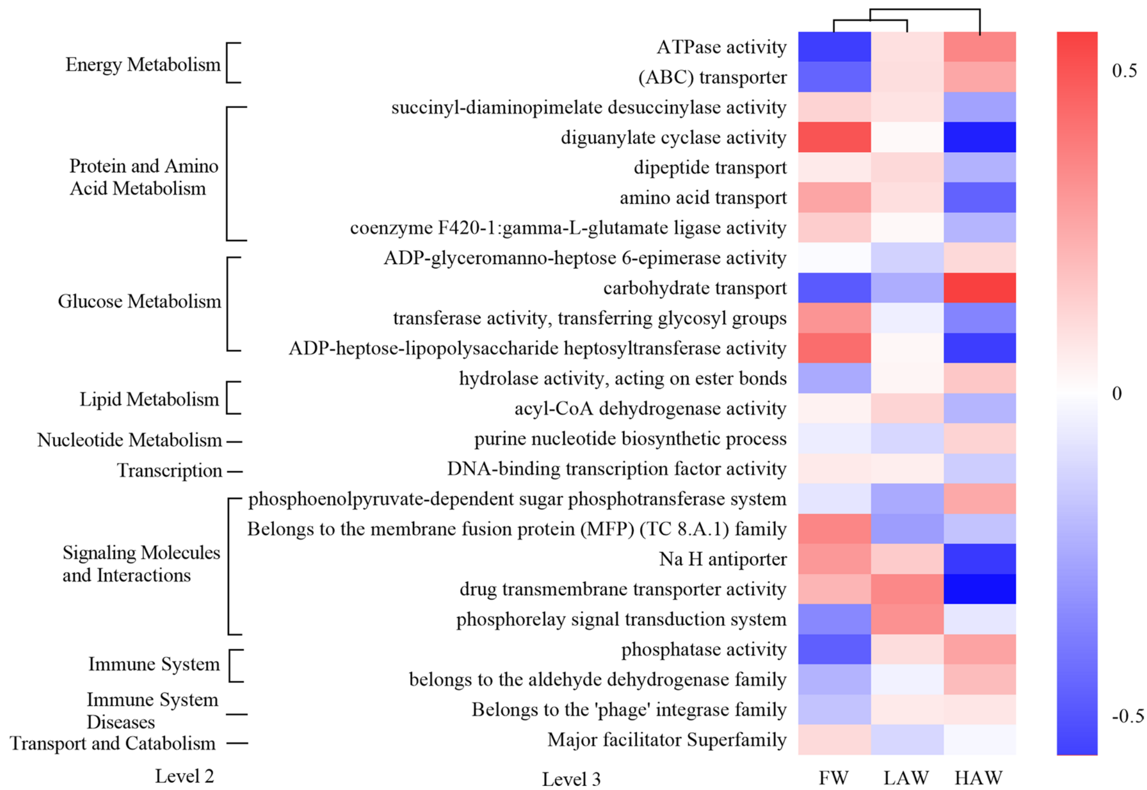

Fig. 9 Distribution of COG functional annotations feature heat maps (*Level 2*, *Level 3*)

in the phosphorelay signal transduction system was higher in the LAW and HAW groups compared to the FW group, with the LAW group having the highest abundance. In the immune system, the abundance of functional flora with phosphatase activity and belonging to the aldehyde dehydrogenase family was higher in the LAW and HAW groups compared to the FW group. The abundance of functional microflora belonging to the phage integrase family in the immune system was lower in the FW group compared to the LAW and HAW groups. The FW group exhibited a higher abundance of functional microflora involved in transport and catabolism compared to the LAW and HAW groups, with the lowest abundance observed in the LAW group.

Discussion

Growth performance, tissue structure, and enzyme activity

In aquaculture, growth performance efficiently reflects the production value and economic benefits of the cultured species (Song et al. 2021). However, environmental factors can play a pivotal role in affecting nutrient uptake, and thus on the growth performance (Yao et al. 2016). In previous studies, it is found that the growth rate of Nile tilapia also showed a decreasing trend with increasing alkalinity (Lin et al. 2013). Intestinal digestive enzyme activity is an important indicator of fish digestion and absorption of feed, and the activity of digestive enzymes reflects the ability of fish to use nutrients (Dawood et al. 2019). In this experiment, $NaHCO_3$ alkaline stress significantly reduced the growth performance and activities of trypsin, amylase, and lipase in juvenile fish. Furthermore, both growth performance and intestinal digestive enzyme activities decreased with increasing alkalinity, while bait coefficients increased accordingly. These findings are consistent with the results obtained from studying different alkalinity conditions in Allogynogemetic crucian carp and *Chalcalburnus chalcoides aralensis* (Bi et al. 2021). The author speculates that there are two reasons. Firstly, in the alkaline environment of juvenile fish, Na^+ ions enter the fish's body, leading to an increase in extracellular osmotic pressure (Cosco et al. 2019). Secondly, K^+, Na^+, and Mg^{2+} present on the external side of proteoliposomes at physiological concentrations inhibit the transport activity. Additionally, OH^- is produced in water during HCO_3^- dehydration, and these OH^- ions enter the intestine, affecting the pH in the intestines of juvenile fish (Zhao et al. 2022). When the osmotic pressure and pH in the intestines of juvenile fish are affected, the activity of intestinal digestive enzymes is reduced, thereby inhibiting the utilization of bait (Wood and Eom 2019). The energy metabolism of fish is directly related to their growth, and an increase in water alkalinity may result in higher energy consumption by juvenile fish to regulate osmotic pressure (Su et al. 2020). As a result, the alkaline environment reduces the allocation of energy towards growth metabolism, decreases bait conversion efficiency, and ultimately impairs the growth performance of grass carp.

Gills serve as the primary organ for material exchange between fish and the external environment, playing a crucial role in osmotic and ionic regulation, acid–base balance, excretion of nitrogenous waste, and facilitating aquatic gas exchange (Evans et al. 2005). Fish gills are also considered as primary target organs for the toxic effects of chemical contaminants. Structural and physiological changes in the gills can serve as effective indicators of water contamination and directly reflect the toxic effects of chemicals on fish (Guo et al. 2022; Tsui et al. 2012). Studies have shown that high water alkalinity, often associated with high pH, results in a decrease in H^+ concentration in fish (Zhao et al. 2022). As a consequence, ammonia nitrogen (NH_3) cannot bind with H^+ and is unable to be excreted in the form of ammonium (NH_4^+) within the body. A high percentage of NH_3 is highly toxic to fish, whereas NH_4^+ is relatively non-toxic. In summary, the elevated pH in alkaline water typically hinders nitrogen waste excretion in fish (Zhao et al. 2020). In this study, it was observed that with increasing alkalinity, the shedding of gill filament interlamellar cell clusters became more pronounced, the spacing between gill lamellae increased, the gill lamellae shortened, the thickness of gill lamellae decreased, and the epithelial cells of gill lamellae were shed in juvenile fish. Firstly, this may be attributed to the dissolution of $NaHCO_3$ in water, which leads to CO_2 dehydration and an increase in PCO_2. As a result, CO_2 can rapidly permeate the cell membrane and easily enter the fish's body (Swietach 2019). This causes a decrease in the pH of the fish's body fluid, a reduction in H^+ concentration, a decrease in the binding of ammonia nitrogen (NH_3) with H^+ in the body, and a decrease in the excretion of NH_3 in the form of ammonia (NH_4^+). Consequently, this leads to ammonia poisoning and respiratory alkalosis in the fish (Brauner et al. 2019; Zhao et al. 2020). Secondly, the entry of Na^+ ions into the blood results in an increase in the osmotic pressure of the extracellular fluid. Additionally, during HCO_3^- dehydration, the concentration of OH^- ions in fish increases, further exacerbating the respiratory alkalosis in the gills of juvenile fish (Zhao et al. 2022). To adapt to the alkaline environment, the epithelial cells of the gill filaments undergo dehydration, leading to the shedding of interlamellar cell masses in the gill filaments, which initially causes an extension of the gill lamellae. As alkalinity continues to increase to 32 mmol/L, the dehydration of gill filament epithelial cells becomes more severe, resulting in the shedding and necrosis of these cells. This leads to a reduction in the length and thickness of gill lamellae, as well as a significant increase in spacing between them. These changes result in a decreased contact area between the gill filaments and the alkaline environment, facilitating physiological adaptation. Eventually, the gill tissue structure exhibits noticeable signs of adaptive degradation.

The liver is an extremely sensitive organ in fish and serves as a vital hub for substance metabolism. It plays a crucial role in the biotransformation of exogenous xenobiotic substances (Eladari and Kumai 2015). It has been observed that an imbalance between the synthesis rate of substances in hepatocytes and their release from the internal circulatory system results in cell vacuolation (Wolf and Wheeler 2018). Alkalinity was the controlled variable in this experiment. The hepatocytes of juvenile fish in the LAW group exhibited enlargement and nucleus deviation from the center of the cell, whereas the hepatocytes of the HAW group displayed cell swelling, nucleus deviation from the center of the cell, and cytoplasmic vacuolation, indicating severe damage. Therefore, the damage to liver cells may be closely related to the metabolic imbalance of Na^+, OH^-, NH_3, and other substances in the liver, which could potentially impair the liver's ability to eliminate harmful metabolites from the body.

The kidney is one of the main metabolic and immune organs of the organism and is very important for regulating osmotic pressure and maintaining homeostasis. Abnormalities in the external environment can lead to corresponding changes in kidney cell structure; therefore, the kidney could be regarded as an indicator of the salinity adaptation range of fish (Handeland et al. 2003). In a study, it was found that the kidney function of *Salmo clarki henshawi* was degraded under hypertonic conditions, with shortened tubules and reduced or even absent glomeruli (Kim et al. 2017). The proximal renal tubule is responsible for most of the renal sodium and bicarbonate reabsorption in tilapia in a bicarbonate environment, and the proximal tubular bicarbonate recycle pathway plays a crucial role in maintaining acid–base balance in tilapia under osmotic stress (Su et al. 2020). The kidneys of grass carp juveniles in the control group exhibited intact kidney cell structure, with no evidence of glomerular structure or significant tubular damage. In contrast, it was observed that the renal tubular lumen in the LAW group was enlarged. Furthermore, the renal tubular epithelial cells in the HAW group exhibited swelling, necrosis, and more pronounced enlargement of the tubular lumen. The author believes that the cause of renal cytopathy is similar to that of gill and liver cells. The decrease in HCO_3^- levels leads to a decrease in the pH of the juvenile fish's body fluids, which in turn reduces the excretion of NH_3 in the form of ammonia (NH_4^+), resulting in metabolic ammonia poisoning in the kidneys. Additionally, this may be attributed to the entry of Na^+ into the kidneys of juvenile fish in highly alkaline water, leading to increased osmotic pressure in the extracellular fluid of the kidneys (Cosco et al. 2019; Jeffries et al. 2019; Zhao et al. 2020). And in order to maintain osmotic pressure balance in the body, the renal tubules may undergo varying degrees of atrophy, which is unfavorable for the excretion of harmful metabolites in juvenile grass carp.

Intestinal microorganisms

The structure of the intestinal flora is closely associated with the host type, diet, individual size, and environment (Sullam et al. 2012). The sequencing results of this experiment revealed that the dominant microflora in the intestines of both the treatment and control groups consisted of Fusobacteria, Proteobacteria, Firmicutes, and Bacteroidetes. These findings were consistent with the dominant microbial flora observed in the intestines of other freshwater fishes, and the proportional structure of the dominant bacterial groups aligned with the results reported by other researchers (Han et al. 2010; Wu et al. 2012). In this experiment, the dominant intestinal flora at the phylum level was relatively similar between the experimental and control groups of juvenile fish. However, there were variations in the abundance of each type of microflora. Specifically, the abundance of Proteobacteria phylum was significantly lower in the LAW and HAW groups compared to the FW group. Proteobacteria is a prominent group in the gut microbial composition of many fish species. For instance, a study by Shaofeng Han (Han et al. 2010) demonstrated that Proteobacteria is the dominant intestinal group in grass carp. The Proteobacteria phylum flora has been found to exhibit a range of metabolic types, with many species being partly anaerobic, heterotrophic, or autotrophic. Additionally, certain species within this phylum possess the capability of utilizing photosynthesis to store energy (Bradley and Pollard 2017). Bacteroidota is a microflora that is involved in sugar metabolism and transport. It has the ability to ferment dietary fiber and decompose various indigestible polysaccharides, thereby providing energy for the host and promoting its growth. The abundance of the Bacteroidota phylum was significantly lower in the HAW group compared to the LAW and FW groups, suggesting that alkalinity negatively impacted the sugar metabolism function of juvenile fish.

The analysis of bacterial composition at the genus level indicated a significant decrease in the abundance of the genus *Cetobacterium* in the HAW group compared to the LAW and FW groups. The genus *Cetobacterium* is known to be a prevalent species found in the intestines of freshwater fish (Casillas et al. 2022). *Cetobacterium* possesses the capability to ferment complex carbohydrates, and a significant population of *Cetobacterium* in the fish intestine is known to produce vitamin B12. Fish are unable to synthesize vitamin B12 internally and depend on external sources to meet their requirements. The primary function of vitamin B12 is to influence DNA synthesis and regulation, participate in cellular metabolism, contribute to fatty acid synthesis, and play a crucial role in energy production. This vitamin plays a key role in maintaining the body's normal hematopoietic process (Casillas et al. 2022; Tsuchiya et al. 2008). In aquatic animals, a deficiency of vitamin B12 can result in reduced appetite in fish (Karmakar et al. 2022). Therefore, the significant decrease in the relative abundance of *Cetobacterium* in the intestinal flora observed in this experiment, caused by alkalinity, may lead to a reduction in vitamin B12 production. Consequently, this could result in decreased appetite in juvenile fish, reduced fulfillment of their nutrient requirements, diminished bait utilization, and hindered growth of the juvenile fish.

The abundance of *Bacteroides* in the HAW group was significantly lower compared to the LAW and FW groups. Research has demonstrated that *Bacteroides* play a beneficial role in enhancing the utilization of nitrogenous substances, biotransformation of steroids, and hydrolysis of macromolecules. Additionally, certain strains of *Bacteroides* can synthesize and secrete polysaccharide A, which possesses anti-inflammatory properties and exhibits a protective effect against liver damage (Hao et al. 2017a, b). It has been discovered that *Bacteroides* are producers of SCFAs (short-chain fatty acids) in the intestine. Elevated levels of SCFAs in the intestine have been linked to the body's inflammatory defense mechanisms. Within the intestinal flora, anthobacteria primarily generate SCFAs such as butyrate and propionate. SCFAs promote melatonin synthesis by decreasing the expression of inducible nitric oxide synthase in the liver and exhibit antioxidant properties. The production of SCFAs activates immune suppressive cells, such as T helper cells, which safeguard the intestinal mucosa against pathogens by diminishing the inflammatory response. This process helps alleviate insulin resistance and inflammation by reducing the release of intestinal toxins (Hao et al. 2017a, b; Wu et al. 2020). Therefore, the fish in the HAW group exhibited a reduced capacity to inhibit the secretion of intestinal toxins, impede inflammatory responses, and maintain antioxidant activity.

Changes in the intestinal environment can lead to altered bacterial growth, and both Na^+ and pH are crucial factors in shaping the gut microbiota (Engevik et al. 2013). The digestive tract is a complex ecosystem, and the internal colonizing bacteria within it carry a greater number of genes compared to the host genome. This allows them to enrich their functional genes within specific signaling pathways through internal restructuring. As a result, they actively participate and influence various aspects of the host's physiological activities, including immunity and nutrition (Zhang et al. 2020). Through clustering analysis of COG functional annotations in the Greengene database, it was observed that the abundance of metabolic functional groups, such as protein metabolism, amino acid metabolism, carbohydrate metabolism, and nucleotide metabolism, was lower in the LAW and HAW groups compared to the FW group. The abundance of these microflora decreases as alkalinity increases, indicating that alkalinity reduces the abundance of flora involved in nutrient digestion and absorption in the intestinal tract of juvenile grass carp. This reduction may lead to a decrease in the intestinal digestion and absorption capacity of grass carp.

In this experiment, the abundance of functional microflora involved in energy metabolism and lipid metabolism was higher in the LAW and HAW groups compared to the FW group. This indicates that grass carp upregulate the abundance of microorganisms associated with lipid and energy metabolism functions in response to the alkaline stress environment. The abundance of functional microflora involved in genetic information processing pathways and cellular transport and catabolism was lower in the LAW and HAW groups compared to the FW group. This indicates that the alkalinity conditions inhibited the growth of functional microflora associated with genetic information processing pathways in grass carp. Consequently, the interaction between the gut microbial community and the gut environment of grass carp is reduced, resulting in decreased participation of gut microorganisms in cellular transport, catabolism, transcription, and translation functions in fish. The abundance of functional flora involved in environmental processing, such as the regulation of iron and potassium homeostasis, sodium, and hydrogen ion transport, signaling, and membrane transport, was lower in the LAW and HAW groups compared to the FW group. This suggests that alkalinity may inhibit the survival of functional flora related to environmental information processing in the intestine, thereby reducing the association of microorganisms with functions related to environmental information processing in the intestine of grass carp. In a study by Barranger et al. (Barranger et al. 2019), it was found that exposure of *Mytilus galloprovincialis* to C_{60} fullerene induces immune and inflammatory responses as a response to stress. These responses include the release of lysozyme, oxidative bursts, and nitric oxide production. Studies have shown that bacteriophages can produce proteins that inhibit the growth of host bacteria (Liu et al. 2004). Aldehyde dehydrogenase plays a role in removing aldehydes from the body and also exhibits catalytic and non-catalytic functions, such as transesterification and oxidative stress (Ziouzenkova et al. 2007). Furthermore, phosphatase activity reflects the physiological activity level and health status of an organism (Lee et al. 2017). In this experiment, the abundance of bacteriophage integrase, aldehyde dehydrogenase, and phosphatase was higher in the LAW and HAW groups of immune organic systems and disease-related functional flora compared to the FW group. These findings indicate that juvenile fish developed defenses under alkalinity conditions, which were countered by gut microbes leading to increased immune enzyme.

Conclusions

This study is the first to investigate the effects of high $NaHCO_3$ alkalinity conditions on the growth performance of juvenile grass carp. In conclusion, the findings indicate that under such conditions, the gills, liver, and kidney tissues of juvenile grass carp are damaged, leading to reduced activity of trypsin, lipase, and amylase. Additionally, the structure and functional status of the intestinal microflora are altered, which may contribute to the decline in the growth performance of grass carp.

Author contribution Jian Wen, Song-Lin Chen, Wen-Ya Xu, Guo-Dong Zheng, and Shu-Ming Zou participated in the conception and design of the study. Jian Wen and Song-Lin Chen analyzed and interpreted the data. Jian Wen and Song-Lin Chen were responsible for drafting the article or revising it critically for important intellectual content. Guo-Dong Zheng and Shu-Ming Zou approved the final version.

Funding Thanks to the following fundings for their strong support and sponsorship of this research: the National Key Research and Development "Blue Granary Technology Innovation" Key Project (grant numbers: 2020YFD0900400), and 32002381 and 32273100 of the National Natural Science Foundation of China.

Data availability The data acquired or analyzed during this investigation are incorporated in this article.

Declarations

Ethics approval All experiments were approved by the institutional review board or ethics committee of Shanghai Ocean University (Permit Number: SHOU-DW-2020-033).

Consent to participate Not applicable

Consent for publication Not applicable

Competing interests The authors declare no competing interests.

References

Barranger A, Langan LM, Sharma V, Rance GA, Aminot Y, Weston NJ, Akcha F, Moore MN, Arlt VM, Khlobystov AN, Readman JW, Jha AN (2019) Antagonistic interactions between benzo pyrene and fullerene (C(60)) in toxicological responseof marine mussels. Nanomaterials-Basel 9:987. https://doi.org/10.3390/nano9070987

Bi B, Gao Y, Jia D, Kong L, Su Y, Rong H, Wu X, Wang X, Hu Z, Hu Q (2021) Growth influence of juvenile golden trout (*Oncorhynchus* *mykiss*) in different osmotic conditions: implications for tissue histology, biochemical indicators, and genes transcription involved in GH/IGF system. Fish Physiol Biochem 47:583–597. https://doi.org/10.1007/s10695-021-00933-w

Bradley PH, Pollard KS (2017) *Proteobacteria* explain significant functional variability in the human gut microbiome. Microbiome 5:1–23. https://doi.org/10.1186/s40168-017-0244-z

Brauner CJ, Shartau RB, Damsgaard C, Esbaugh AJ, Grosell MJ (2019) Acid-base physiology and CO_2 homeostasis: regulation and compensation in response to elevated environmental CO_2. Fish Physiol 37:69–132. https://doi.org/10.1016/bs.fp.2019.08.003

Casillas HR, Gonzalez-Galaviz JR, Rodriguez-Anaya LZ, Gil-Nunez JC, Rodriguez-Jaramillo MDC (2022) Dietary use of methionine sources and *bacillus amyloliquefaciens* CECT 5940 influences growth performance, hepatopancreatic histology, digestion, immunity, and digestive microbiota of *Litopenaeus vannamei* fed reduced fishmeal diets. Animals -Basel 13:43. https://doi.org/10.3390/ani13010043

Chen SA, Hou J, Yao N, Xie C, Li D (2020) Comparative transcriptome analysis of *Triplophysa yarkandensis* in response to salinity and alkalinity stress. Comp Biochem Phys D 33:100629. https://doi.org/10.1016/j.cbd.2019.100629

Cosco J, Regina T, Scalise M, Galluccio M, Indiveri C (2019) Regulatory aspects of the vacuolar CAT2 arginine transporter of S lycopersicum: role of osmotic pressure and cations. Int J Mol Sci 20:906. https://doi.org/10.3390/ijms20040906

Dawood MAO, Magouz FI, Mansour M, Saleh AA, Asely A, Fadl SE, Ahmed HA, Al-Ghanim KA, Mahboob S, Al-Misned F (2019) Evaluation of yeast fermented poultry by-product meal in Nile Tilapia (*Oreochromis niloticus*) feed: effects on growth performance, digestive enzymes activity, innate immunity, and antioxidant capacity. Front Vet Sci 6:516. https://doi.org/10.3389/fvets.2019.00516

Eladari D, Kumai Y (2015) Renal acid-base regulation: new insights from animal models. Pflugers Arch Eur J Phy 467:1623–1641. https://doi.org/10.1007/s00424-014-1669-x

Engevik MA, Aihara E, Montrose MH, Shull GE, Hassett DJ, Worrell RT (2013) Loss of NHE3 alters gut microbiota composition and influences *Bacteroides thetaiotaomicron* growth. Am J Physiol 305:G697–G711. https://doi.org/10.1152/ajpgi.00184.2013

Evans DH, Piermarini PM, Choe KP (2005) The multifunctional fish gill: dominant site of gas exchange, osmoregulation, acid-base regulation, and excretion of nitrogenous waste. Physiol Rev 85:97–177. https://doi.org/10.1152/physrev.00050.2003

Ge Q, Li J, Wang J, Li Z, Li J (2019) Characterization, functional analysis, and expression levels of three carbonic anhydrases in response to pH and saline-alkaline stresses in the ridgetail white prawn *Exopalaemon carinicauda*. Cell Stress Chaperones 24:503–515. https://doi.org/10.1007/s12192-01900987-z

Guo H, Kuang Y, Ouyang K, Zhang C, Yang H, Chen S, Tang R, Zhang X, Li D, Li L (2022) Ammonia in the presence of nano titanium dioxide (nanoTiO_2) induces greater oxidative damage in the gill and liver of female zebrafish. Ecotoxicol Environ Saf 236:113458. https://doi.org/10.1016/j.ecoenv.2022.113458

Han SF, Liu YC, Zhou ZG, He SX, Cao YA, Shi PJ, Yao B, Einar R (2010) Analysis of bacterial diversity in the intestine of grass carp (*Ctenopharyngodon idellus*) based on 16S rDNA gene sequences. Aquacult Res 42:47–56. https://doi.org/10.1111/j.1365-2109.2010.02543.x

Handeland SO, Arnesen AM, Stefansson SO (2003) Seawater adaptation and growth of post-smolt Atlantic salmon (*Salmo salar*) of wild and farmed strains. Aquaculture 220:367–384. https://doi.org/10.1016/S0044-8486(02)00508-2

Hao YT, Wu SG, Xiong F, Tran NT, Jakovlic I, Zou H, Li WX, Wang GT (2017a) Succession and fermentation products of grass carp (*Ctenopharyngodon idellus*) hindgut microbiota in response to an extreme dietary shift. Front Microbiol 8:1585. https://doi.org/10.3389/fmicb.2017.01585

Hao YT, Wu SG, Jakovlic I, Zou HL, Wen X, Wang GT (2017b) Impacts of diet on hindgut microbiota and short-chain fatty acids in grass carp (*Ctenopharyngodon idellus*). Aquacult Res 48:5595–5605. https://doi.org/10.1111/are.13381

Hassenruck C, Reinwald H, Kunzmann A, Tiedemann I, Gardes A (2020) Effects of thermal stress on the gut microbiome of juvenile milkfish (*Chanos chanos*). Microorganisms 9:5. https://doi.org/10.3390/microorganisms9010005

Jeffries KM, Connon RE, Verhille CE, Dabruzzi TF, Britton MT, Durbin-Johnson BP, Fangue NA (2019) Divergent transcriptomic signatures in response to salinity exposure in two populations of an estuarine fish. Evol Appl 12:1212–1226. https://doi.org/10.1111/eva.12799

Karmakar S, Sen GP, Bhattacharya S, Sarkar A, Rahaman A, Mandal DP, Bhattacharjee S (2022) Vitamin B12 alleviates malathion-induced toxicity in zebra fish by regulating cytochromeP450 and PgP expressions. Toxicol Mech Methods 24:1–14. https://doi.org/10.1080/15376516.2022.2145590

Kim JH, Park HJ, Kim KW, Hwang IK, Kim DH, Lee JS, Kang JC (2017) Growth performance, oxidative stress, and non-specific immune responses in juvenile sablefish, *Anoplopomafimbria*, by changes of water temperature and salinity. Fish Physiol Biochem 43:1421–1431. https://doi.org/10.1007/s10695-017-0382-z

Kobyliak N, Conte C, Cammarota G, Haley AP, Styriak I, Gaspar L, Fusek J, Rodrigo L, Kruzliak P (2016) Probiotics in prevention and treatment of obesity: a critical view. Nutr Metab 13:1–13. https://doi.org/10.1186/s12986-016-0067-0

Lee YC, Su CY, Lin YF, Lin CM, Fang CY, Lin YK, Hsiao M, Chen O (2017) Lysosomal acid phosphatase 2 is an unfavorable prognostic factor but is associated with better survival in stage II colorectal cancer patients receiving chemotherapy. Oncotarget 8:12120–12132. https://doi.org/10.18632/oncotarget.14552

Lin T, Lai Q, Yao Z, Lu J, Zhou K, Wang H (2013) Combined effects of carbonate alkalinity and pH on survival, growth and haemocyte parameters of the venus clam *Cyclina sinensis*. Fish Shellfish Immunol 35:525–531. https://doi.org/10.1016/j.fsi.2013.05.006

Liu J, Dehbi M, Moeck G, Arhin F, Bauda P, Bergeron D, Callejo M, Ferretti V, Ha N, Kwan T (2004) antimicrobial drug discovery through bacteriophage genomics. Nat Biotechnol 22:185–191. https://doi.org/10.1038/nbt93

Song LY, Zhao Y, Song YD, Zhao LL, Ma CX, Zhao JL (2021) Effects of saline-alkaline water on growth performance, nutritional processing, and immunity in Nile tilapia (*Oreochromis niloticus*). Aquaculture 544:737036. https://doi.org/10.1016/j.aquaculture.2021.737036

Su H, Ma D, Zhu H, Liu Z, Gao F (2020) Transcriptomic response to three osmotic stresses in gills of hybrid tilapia (*Oreochromis mossambicus female* × *O. urolepis hornorum male*). BMC Med Genomics 21:1–20. https://doi.org/10.1186/s12864-020-6512-5

Sullam KE, Essinger SD, Lozupone CA, Connor MP, Rosen GL, Knight R, Kilham SS, Russell JA (2012) Environmental and ecological factors that shape the gut bacterial communities of fish: a meta-analysis. Mol Ecol 21:3363–3378. https://doi.org/10.1111/j.1365-294X.2012.05552.x

Swietach P (2019) What is pH regulation, and why do cancer cells need it? Cancer Metastasis Rev 38:5–15. https://doi.org/10.1007/s10555-018-09778-x

Tsuchiya C, Sakata T, Sugita H (2008) Novel ecological niche of *Cetobacterium* somerae, an anaerobic bacterium in the intestinal tracts of freshwater fish. Lett Appl Microbiol 46:43–48. https://doi.org/10.1111/j.1472-765X.2007.02258.x

Tsui WC, Chen JC, Cheng SY (2012) The effects of a sudden salinity change on cortisol, glucose, lactate, and osmolality levels in grouper *Epinephelus malabaricus*. Fish Physiol Biochem 38:1323–1329. https://doi.org/10.1007/s10695-012-9620-6

Wolf JC, Wheeler JR (2018) A critical review of histopathological findings associated with endocrine and non-endocrine hepatic toxicity in fish models. Aquat Toxicol 197:60–78. https://doi.org/10.1016/j.aquatox.2018.01.013

Wood CM, Eom J (2019) The internal CO_2 threat to fish: high PCO_2 in the digestive tract. Proc R Soc B 286:1907. https://doi.org/10.1098/rspb.2019.0832

Wu S, Wang G, Angert ER, Wang W, Li W, Zou H (2012) Composition, diversity, and origin of the bacterial community in grass carp intestine. PLoS One 7:e30440. https://doi.org/10.1371/journal.pone.0030440

Wu M, Yang S, Wang S, Cao Y, Zhao R, Li X, Xing Y, Liu L (2020) Effect of berberine on atherosclerosis and gut microbiota modulation and their correlation in high-fat diet-fed ApoE-/- mice. Front Pharmacol 11:223. https://doi.org/10.3389/fphar.2020.00223

Yang G, Zhao W, Qin C, Yang L, Meng X, Lu R, Yan X, Cao X, Zhang Y, Nie G (2020) Molecular identification of grass carp *igfbp2* and the effect of glucose, insulin, and glucagon on *igfbp2* mRNA expression. Fish Physiol Biochem 46:1469–1482. https://doi.org/10.1007/s10695-020-00804-w

Yao ZL, Wang H, Chen L, Zhou K, Ying CQ, Lai QF (2012) Transcriptomic profiles of Japanese medaka (*Oryzias latipes*) in response to alkalinity stress. GMR Genet Mol Res 11:2200–2246. https://doi.org/10.4238/2012.June.15.2

Yao Z, Lai Q, Hao Z, Chen L, Lin T, Zhou K, Wang H (2015) Carbonic anhydrase 2-like and Na^+-K^+-ATPase α gene expression in medaka (*Oryzias latipes*) under carbonate alkalinity stress. Fish Physiol Biochem 41:1491–1500. https://doi.org/10.1007/s10695-015-0101-6

Yao Z, Guo W, Lai Q, Shi J, Zhou K, Qi H, Lin T, Li Z, Wang H (2016) *Gymnocypris przewalskii* decreases cytosolic carbonic anhydrase expression to compensate for respiratory alkalosis and osmoregulation in the saline-alkaline lake Qinghai. J Comp Physiol, B 186:83–95. https://doi.org/10.1007/s00360-015-0939-z

Yi Y, Liang L, Wang Z, Ai P, You X, Bian C, Shi Q, Dong B (2019) A comparative metagenomics study on gastrointestinal microbiota in amphibious mudskippers and other vertebrate animals. Animals 9:660. https://doi.org/10.3390/ani9090660

Zhang ML, Li M, Sheng Y, Tan F, Chen L, Cann I, Du ZY (2020) *Citrobacter* species increase energy harvest by modulating intestinal microbiota in fish: nondominant species play important functions. mSystems 5:e00303-20. https://doi.org/10.1128/mSystems.00303-20

Zhao Y, Zhang CS, Zhou HT, Song LY, Wang J, Zhao JL (2020) Transcriptome changes for Nile tilapia (*Oreochromis niloticus*) in response to alkalinity stress. Comp Biochem Physiol, Part D: Genomics Proteomics 33:100651. https://doi.org/10.1016/j.cbd.2019.100651

Zhao Y, Wang Y, Zhang C, Zhou H, Song L, Tu H, Zhao J (2022) Variation in pH, HCO3, carbonic anhydrases, and HCO3 transporters in Nile tilapia during carbonate alkalinity stress. Hydrobiologia 850:2447–2459. https://doi.org/10.1007/s10750-022-05020-6

Ziouzenkova O, Orasanu G, Sharlach M (2007) Retinaldehyde represses adipogenesis and dietinduced obesity. Nat Med 13:695–702. https://doi.org/10.1038/nm1587